



TITLE:

Deep-ultraviolet micro-Raman investigation of surface defects in a 4H-SiC homoepitaxially grown film

AUTHOR(S):

Tomita, Takuro; Matsuo, Shigeki; Okada, Tatsuya; Kimoto, Tsunenobu; Matsunami, Hiroyuki; Mitani, Takeshi; Nakashima, Shin-Ichi

CITATION:

Tomita, Takuro ...[et al]. Deep-ultraviolet micro-Raman investigation of surface defects in a 4H-SiC homoepitaxially grown film. AA00543431 2005, 87(24): 241906.

ISSUE DATE:

2005-12-12

URL:

<http://hdl.handle.net/2433/24190>

RIGHT:

Copyright 2005 American Institute of Physics. This article may be downloaded for personal use only. Any other use requires prior permission of the author and the American Institute of Physics.

Deep-ultraviolet micro-Raman investigation of surface defects in a 4H-SiC homoepitaxially grown film

Takuro Tomita^{a)} and Shigeki Matsuo

Department of Ecosystem Engineering, The University of Tokushima, Tokushima 770-8506, Japan

Tatsuya Okada

Department of Mechanical Engineering, The University of Tokushima, Tokushima 770-8506, Japan

Tsunenobu Kimoto and Hiroyuki Matsunami

Department of Electronic Science and Engineering, Kyoto University, Kyoto 615-8510, Japan

Takeshi Mitani and Shin-Ichi Nakashima

National Institute of Advanced Industrial Science and Technology, Tsukuba Central 2, Ibaraki 305-8568, Japan

(Received 14 April 2005; accepted 16 October 2005; published online 6 December 2005)

The structures of comet defects in a 4H-SiC homoepitaxially grown film are investigated by deep-ultraviolet micro-Raman spectroscopy. Spatial distribution of the 4H- and 3C-SiC is clearly distinguished both from the intensities of the folded longitudinal acoustic phonon mode and the peak energies of the nonfolded longitudinal optical phonon mode. The mappings of these parameters indicate the existence of two types of comets. The mechanisms of heteropolytypic inclusion in comets are discussed. © 2005 American Institute of Physics. [DOI: [10.1063/1.2142080](https://doi.org/10.1063/1.2142080)]

Silicon carbide (SiC) is a promising material for the high-power, high-temperature, and high-speed devices, because of its wide valence to conduction band gap.^{1–5} When the SiC Schottky diodes having kV-class blocking voltage are fabricated, their ON-resistance will be lowered by at least two orders of magnitude than that of similar devices made of silicon. This leads to the drastic reduction in power consumption of the diode. In the homoepitaxial growth of 4H-SiC films, however, the unintentionally produced defects called “comets” considerably degrade the breakdown voltage of SiC diode. Thus, comets are regarded as the device-killing defects. Although recent progress in the growth techniques have drastically reduced the density of comets in the films homoepitaxially grown on (0001) 8°-off wafers, comets in the films homoepitaxially grown on the 3.5°-off or nearly on-axis wafers still have been observed and gives the serious effect on electrical properties.

Some studies of heteropolytypic inclusion in the homoepitaxially grown films have been reported.^{6,7} Recently, Okada *et al.* reported the observations of comets by conventional transmission electron microscopy (TEM).⁸ While TEM provides information on defect structure with an atomic scale resolution, it needs the sample destruction and needs much time and efforts. Thus, the nondestructive measurements and the statistical analysis of comets are almost impossible by TEM. In addition, TEM observation can reveal only the symmetry of crystal structure, but the determination of long range order is impossible by TEM observation from *c*-axis direction.

Because the Raman measurement gives the energies of phonon modes characteristic of polytypes, it is possible to distinguish every polytypes regardless of their symmetries. Although several groups tried to measure the micro-Raman spectra on the surface defects in epitaxially grown SiC films, they have failed to observe the spectrum of 3C-SiC in

comets.^{9,10} Because of the deep penetration depth of the visible laser line ($>200\text{ }\mu\text{m}$ for 3C-SiC and $\geq 1\text{ cm}$ for 4H-SiC at 488 nm wavelength¹¹), 3C-SiC which exists only near the surface ($<9\text{ }\mu\text{m}$) was not detected.

In this letter, we will report the results of deep-ultraviolet (DUV) micro-Raman measurements of comets. The penetration depth at the wavelength of a 244 nm laser is about 100 nm for SiC. This enables us to obtain the Raman spectra only from the near-surface of SiC. In addition, selective resonance effect in ultraviolet region, which enhances the Raman intensities of folded phonon modes of SiC, helps us to distinguish the polytype structures.¹² Thus, DUV micro-Raman spectroscopy is a powerful tool for investigating the surface defects and the microstructures of surfaces. The microstructural analysis of heteropolytypic inclusion can give information about formation mechanisms of heteropolytypic layers.

The light source used in this experiment was an intracavity frequency-doubled Ar⁺ laser operated at 244 nm (Coherent 300C FreD). The laser beam was guided into the microscope and focused by a Cassegrain objective. The spatial resolution of this measurement was about 10 μm . The measurements were done in the backscattering geometry. The scattered light was filtered by a subtractive double monochromator (Photon design), then spectrum was detected by a single spectrometer (Sopra UHRS F1500) with a liquid nitrogen cooled charge coupled device detector (Roper Scientific Spec-10:256e/In).^{13–15} The experimental error of this detection system is about 1 cm^{-1} . The details of this experimental setup were described in Ref. 13. The sample used in this experiment was a 4H-SiC epitaxially grown film with a thickness of 9 μm which was grown on an *n*-type substrate by chemical vapor deposition in a $\text{SiH}_4\text{--C}_3\text{H}_8\text{--H}_2$ system at 1500 °C.¹⁶ For the growth of the homoepitaxial film, the step-controlled epitaxy was adopted. The substrate of this film was a 4H-SiC single crystal wafer off-cut (off-oriented) from the exact (0001) plane by 8°, while keeping projection of the $[11\bar{2}0]$ direction.⁸

^{a)}Electronic mail: tomita@eco.tokushima-u.ac.jp

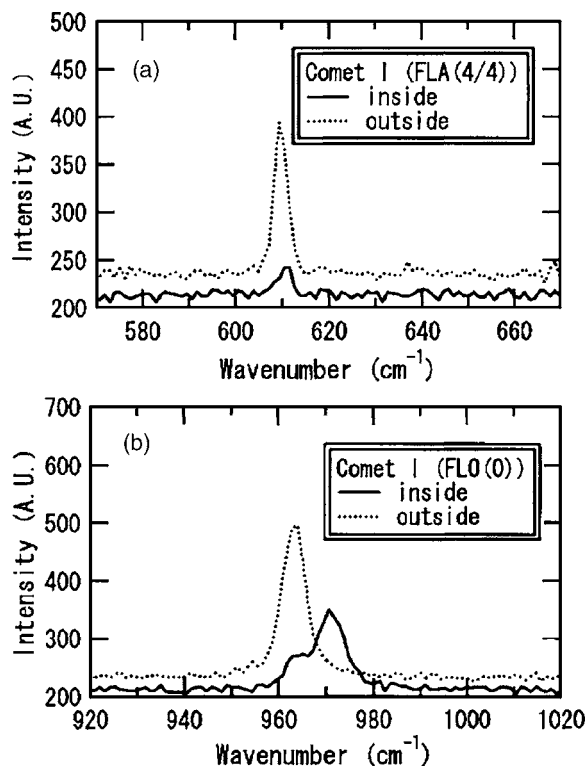


FIG. 1. The Raman spectra of the 4H-SiC epitaxially grown film around the comet I are plotted. The solid and dotted lines correspond to the spectra at the inside and the outside of the comet I, respectively. The spectra are shifted along the ordinate for a convenient display. The intensity of the FLA(4/4) mode is much smaller and the energies of the FLO(0) mode is higher at the inside of the comet I.

DUV micro-Raman spectra for a comet are shown in Fig. 1. The solid line correspond to the spectrum at the inside of the comet, and the dotted line corresponds to the spectrum at the outside of it. The peak energies and the intensities of FLA(4/4) mode¹⁷ of the spectrum at the outside of the comet agree well with those of the bulk 4H-SiC. However, the spectrum at the inside of it differs from that of 4H-SiC. Here, FLO (FLA) stands for a folded longitudinal optical (acoustic) phonon mode and FTO (FTA) stands for a folded transverse optical (acoustic) mode. The energies of the FLO(0) mode of the inside was higher than that of the outside by 8 cm^{-1} and the intensities of the FLA(4/4) mode was drastically lower at the inside of the comet. Although the results are not shown in Fig. 1, the intensity of FTO(0) mode was also much higher at the inside of the comet. These differences clearly indicate the presence of 3C-SiC at the inside of the comet. While the peak energies of the FLO(0) mode and the intensities of the FLA(4/4) mode are different, the difference of spectral shapes could not be detected for all the probed area. These results indicate that the interface between 3C- and 4H-SiC regions is abrupt. The existence of stacking faults around the interface could not be detected. In the spectrum of 3C-SiC, the small contribution of 4H-SiC was also observed. This is because the spatial resolution of this experiment was relatively larger than the structure of comet.

In order to examine the spatial distribution of polytypes, Raman spectra were measured from the top to the tail of the comets. Here, we introduce the normalized scale to specify the position of probed spot. In Fig. 2(a), an optical micrograph of a comet is shown. The normalized scale is shown under the comet; the top and the end of the comet is set to 0

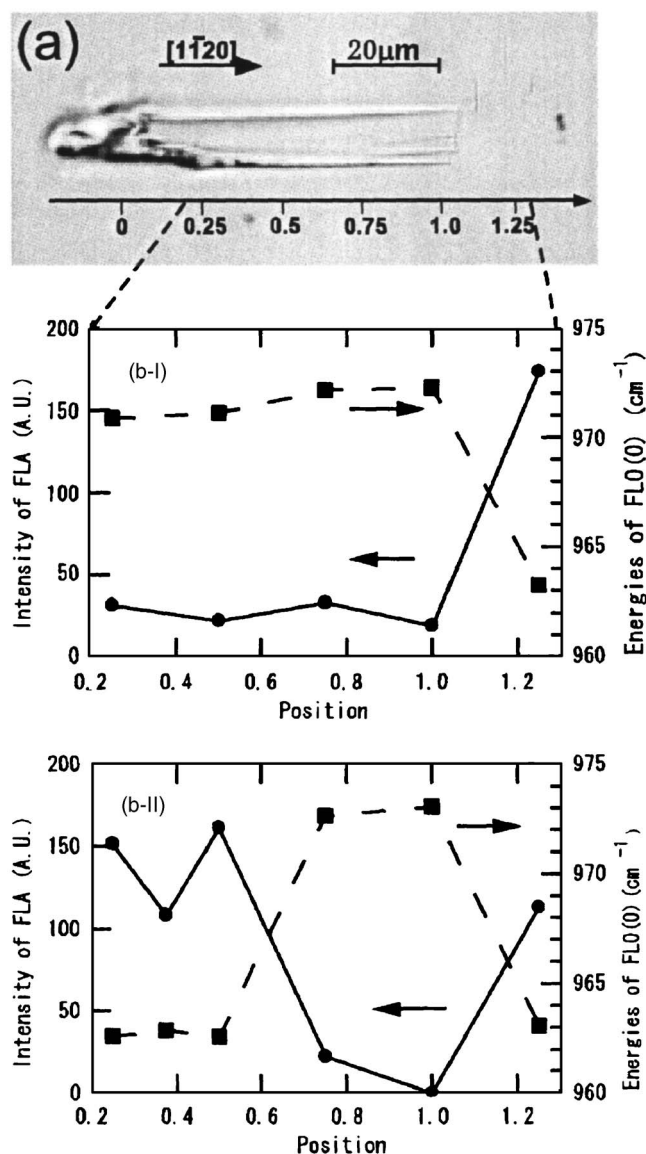


FIG. 2. (a) The optical micrograph of a comet I is shown. The normalized scale is shown under the comet; the top and the end of the comet is set to 0 and 1, respectively. (b) The intensities of the FLA(4/4) mode and the peak energy of the FLO(0) mode are plotted as a function of the position of the probed spot. The plot (b-I) is for the comet I and the (b-II) is for the comet II.

and 1, respectively. The Raman spectra just on the top of comets (normalized position is 0) were not measured because of the rough surface.

We have measured the position dependence of Raman spectra for seven comets. The position dependence of Raman spectra in comets can be classified into two types: types I and II. In Fig. 2, we will show the two types of position dependence as a function of normalized position for comet I (type I) and comet II (type II). In the following, we will focus on the intensities of the FLA(4/4) mode and the energies of the FLO(0) mode for simplicity. In Fig. 2(b), the intensities of the FLA(4/4) mode and the energies of the FLO(0) mode are plotted as a function of normalized position. Figure 2(b-I) shows the results for the comet I (type I), and Fig. 2(b-II) shows the results for the comet II (type II). In these figures, the intensities of the FLA(4/4) mode are plotted by filled circles with solid lines and the energies of the FLO(0) mode are plotted by filled squares with broken lines.

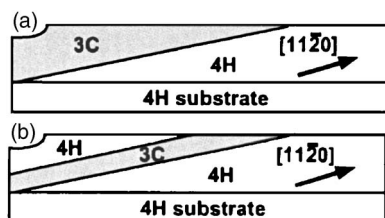


FIG. 3. The estimated cross sections in the $(1\bar{1}00)$ plane are shown for the comet I (a) and the comet II (b).

In Fig. 2(b-I), the intensities of the FLA(4/4) mode are about 30 around the normalized position of 0.25–1.0 in the comet I and increase up to about 170 at the normalized position of 1.25. The energies of the FLO(0) mode also changes from 972 to 964 cm^{-1} at the normalized position of 1.25. The energies of the FLO(0) mode for 3C- and 4H-SiC were reported to be 972 and 964 cm^{-1} , respectively.¹⁸ Our results agree fairly well with these reported values. These results indicate that the 3C-SiC is included in a whole area of the inside of comet I.

In Fig. 2(b-II), the intensity of the FLA(4/4) mode is about 150 around the normalized position of 0.2–0.5 in the comet II and decrease to around 20 at the normalized position of 0.8–1.0 and increase again up to about 110 at the normalized position of 1.25. Similarly, the energies of the FLO(0) mode also changed from 963 to 973 cm^{-1} about 0.8 to 1.0. These results indicate that the 3C-SiC is included around the tail of the comet II.

In the following, we will discuss two polytype distributions in the interior of comets. Schematic structures of these two comets viewed in $(1\bar{1}00)$ cross section are shown in Figs. 3(a) and 3(b). Figure 3(a) and 3(b) corresponds to comet I and comet II, respectively. All the interior of comet I is 3C-SiC. In contrast, in comet II, 3C-SiC is sandwiched between two 4H-SiC layers and the 3C-SiC is observed around the tail of comet near the surface. These results are consistent with the previous report by Okada *et al.*⁸ In comet II, the width of 3C-SiC layer in the surface region determined from DUV Raman measurements is about 20 μm . Thus, the thickness of the 3C-SiC layers estimated from this value is about 2.8 μm ($\sim 20 \mu\text{m} \times \sin 8^\circ$).

As mentioned earlier, we measured the DUV micro-Raman spectra on seven comets. We confirmed the existence of 3C-SiC near the surface of comets by DUV Raman spectroscopy. We found that all the comets can be classified into types I or II. Other types of distribution and other polytype inclusions except for 3C- and 4H-SiC were not found in these comets. In our measurement, six of seven comets were type I and one of seven comets was type II.

Hallin *et al.* reported the 3C-SiC inclusion in triangular stacking faults (TSFs).⁶ The reported width of sandwiched 3C-SiC layer is 80 nm for TSFs. They concluded that the 3C inclusion is caused by the stacking faults. In comets, however, the included 3C layer is much thicker than that of TSFs, and most of the comets include 3C all inside of it (type I). These thick 3C inclusions cannot be explained by the stacking faults due to the electronic origin. The possible origin of comets is the anomalous growth of 3C layers that are caused by the point defects or the inclusions on the surface of substrate. These nucleuses on the surface disturb the flow of growth gases. As the growth conditions are changed due to the disturbed flow, the heteropolytypic growth will be caused. In other words, comets will be generated by this disturbed flow in the homoepitaxially grown films.

In conclusion, DUV micro-Raman spectra were measured for comets on the 4H-SiC homoepitaxially grown film. At the inside of the comets, the spectra of 3C-SiC was observed. It was also found that the polytype distribution of comets is classified into two. The thickness of 3C-SiC layers is determined from the measurement, and the formation mechanism of heteropolytypic inclusion in comets is discussed. Our results demonstrated that the DUV micro-Raman spectroscopy is a powerful tool for investigating the surface structures and surface defects.

¹T. Kimoto, T. Urushidani, S. Kobayashi, and H. Matsunami, IEEE Electron Device Lett. **14**, 548 (1993).

²S. Onda, R. Kumar, and K. Hara, Phys. Status Solidi A **162**, 369 (1997).

³W. von Muench and E. Pettenpaul, J. Appl. Phys. **48**, 4823 (1997).

⁴W. von Muench and I. Pfaffeneder, J. Appl. Phys. **48**, 4831 (1997).

⁵G. A. Slack, J. Appl. Phys. **35**, 3460 (1964).

⁶C. Hallin, A. O. Konstantinov, B. Pécz, O. Kordina, and E. Janzén, Diamond Relat. Mater. **6**, 1297 (1997).

⁷A. Fissel, B. Schröter, U. Kaiser, and W. Richter, Appl. Phys. Lett. **77**, 2418 (2000).

⁸T. Okada, T. Kimoto, K. Yamai, H. Matsunami, and F. Inoko, Mater. Sci. Eng., A **361**, 67 (2003).

⁹L. Scaltrito, S. Porro, M. Cocuzza, F. Giorgis, C. F. Pirri, P. Mandracchi, C. Ricciardi, S. Ferrero, C. Sgorlon, G. Richieri, L. Merlin, A. Castaldini, A. Cavallini, and L. Polenta, Mater. Sci. Eng., B **102**, 298 (2003).

¹⁰C. Sarte, C. Balloud, V. Soulière, S. Juillaguet, J. Dazord, Y. Monteil, J. Camassel, and S. Rushworth, Mater. Sci. Forum **457–460**, 217 (2004).

¹¹H. R. Philipp, Phys. Rev. **111**, 440 (1958).

¹²T. Tomita, S. Saito, M. Baba, M. Hundhausen, T. Suemoto, and S. Nakashima, Phys. Rev. B **62**, 12896 (2000).

¹³S. Nakashima, H. Okumura, T. Yamamoto, and R. Shimizu, Appl. Spectrosc. **58**, 224 (2004).

¹⁴S. Nakashima, J. Phys.: Condens. Matter **16**, S25 (2004).

¹⁵S. Nakashima, T. Yamamoto, A. Ogura, K. Uejima, and T. Yamamoto, Appl. Phys. Lett. **84**, 2533 (2004).

¹⁶H. Matsunami and T. Kimoto, Mater. Sci. Eng., R. **20**, 125 (1997).

¹⁷In this report, according to the precedent, we will denote the folded transverse (longitudinal) acoustic and optical phonon modes as FTA (FLA) and FTO (FLO), respectively. The number in the parentheses is the reduced wave vector of the corresponding phonon in the Brillouin zone of 3C-SiC.

¹⁸S. Nakashima and H. Harima, Phys. Status Solidi A **162**, 39 (1997).